Title

The basic helix-loop-helix transcription factor, heart and neural crest derivatives expressed transcript 2, marks hepatic stellate cells in zebrafish: Analysis of stellate cell entry into the developing liver

Journal

Hepatology, 56(5)

ISSN

0270-9139

Authors

Yin, Chunyue
Evason, Kimberley J
Maher, Jacquelyn J
et al.

Publication Date

2012-11-01

DOI

10.1002/hep.25757

Peer reviewed

Published in final edited form as:
Hepatology. 2012 November ; 56(5): 1958–1970. doi:10.1002/hep.25757.

The bHLH Transcription Factor Hand2 Marks Hepatic Stellate Cells in Zebrafish: Analysis of Stellate Cell Entry into the Developing Liver

Chunyue Yin[1,4], **Kimberley J. Evason**[1,2,4], **Jacquelyn J. Maher**[3], and **Didier Y.R. Stainier**[1]

[1]Department of Biochemistry and Biophysics, Programs in Developmental and Stem Cell Biology, Genetics and Human Genetics, Liver Center and Diabetes Center, Institute for Regeneration Medicine, University of California, San Francisco, CA 94158, USA.

[2]Department of Pathology, University of California, San Francisco, CA 94143, USA.

[3]Department of Medicine, and Liver Center, University of California, San Francisco, CA 94110, USA.

Abstract

Hepatic stellate cells (HSCs) are liver-specific mesenchymal cells that play vital roles in liver development and injury. Our knowledge of HSC biology is limited by the paucity of *in vivo* data. HSCs and sinusoidal endothelial cells (SECs) reside in close proximity and interactions between these two cell types are potentially critical for their development and function. Here we introduce a transgenic zebrafish line, *Tg(hand2:EGFP)*, that labels HSCs. We find that zebrafish HSCs share many similarities with their mammalian counterparts, including morphology, location, lipid storage, gene expression profile, and increased proliferation and matrix production in response to an acute hepatic insult. Using the *Tg(hand2:EGFP)* line, we conducted time course analyses during development to reveal that HSCs invade the liver after SECs do. However, HSCs still enter the liver in mutants that lack most endothelial cells including SECs, indicating that SECs are not required for HSC differentiation or their entry into the liver. In the absence of SECs, HSCs become abnormally associated with hepatic biliary cells, suggesting that SECs influence HSC localization during liver development. We analyzed factors that regulate HSC development and show that inhibition of vascular endothelial growth factor signaling significantly reduces the number of HSCs that enter the liver. We also performed a pilot chemical screen and identified two compounds that affect HSC numbers during development.

Conclusion—Our work provides the first comprehensive description of HSC development in zebrafish and reveals the requirement of SECs in HSC localization. The *Tg(hand2:EGFP)* line represents a unique tool for *in vivo* analysis and molecular dissection of HSC behavior.

Keywords

sinusoidal endothelial cells; liver development; *cloche*; VEGF; biliary cells; acute alcohol exposure

Contact information: Didier Y.R. Stainier, Ph.D., or Chunyue Yin, Ph.D., Department of Biochemistry and Biophysics, Programs in Developmental and Stem Cell Biology, Genetics and Human Genetics, Liver Center and Diabetes Center, Institute for Regeneration Medicine, University of California, San Francisco. 1550 Fourth Street, Room 384, San Francisco, CA 94158, USA. Didier.stainier@ucsf.eduChunyue.yin@ucsf.edu Telephone: 1-415-502-5680. Kimberley J. Evason: Kimberley.Evason@ucsfmedctr.org Jacquelyn J. Maher: jmaher@medsfgh.ucsf.edu.
[4]These authors contribute equally to this work.

Hepatic stellate cells (HSCs) represent a versatile mesenchymal cell type that plays vital roles in liver function and injury response. In healthy livers, HSCs serve as the main vitamin A-storing cells. Upon liver injury, these quiescent cells transform into activated, proliferative myofibroblast-like cells to generate scar tissue (reviewed by 1). Sustained activation of HSCs is a central event in liver fibrosis and has been linked to the progression of hepatitis and steatohepatitis (reviewed by 2).

Despite the importance of HSCs in liver physiology and disease, our knowledge of HSC biology is far from complete. Characterization of HSC development could provide clues for understanding their activation during liver injury. However, tracking HSCs during development has not yet been feasible in mammalian models. The embryonic origin of HSCs is elusive because they express marker genes of all three germ layers (3, 4). Genetic lineage-tracing analysis in mice using a *CreERT2* transgene knocked into the *Wilms' tumor suppressor (Wt1)* locus indicated that HSCs derive from the septum transversum-derived mesothelium (5). Interestingly, in chick, the mesothelium contributes not only to HSCs, but also to sinusoidal endothelial cells (SECs) (6). HSCs and SECs exhibit close physical association and common expression of angiogenic factors (7). These observations have led to the hypothesis that HSCs and SECs originate from a common embryonic precursor. However, no studies have specifically addressed this issue.

Finding promoters that selectively drive transgene expression in HSCs could facilitate both their *in vivo* observation and their genetic manipulation. Previous studies used the promoters of the mesoderm-associated α*-smooth muscle actin* gene and the neural crest-related *glial fibrillary acidic protein/GFAP* gene to direct gene expression in HSCs in transgenic mice (8-10). However, identifying HSC-specific promoters remains challenging. The bHLH transcription factor gene heart and neural crest derivatives expressed transcript 2/*hand2* is expressed in the lateral plate mesoderm and the neural crest (11), tissues that may give rise to HSCs. We previously reported the generation of the *Tg(hand2:EGFP)* zebrafish line that expresses EGFP under the control of the *hand2* regulatory sequences (12). During liver budding morphogenesis, *Tg(hand2:*EGFP) is expressed in the lateral plate mesoderm surrounding the liver primordium. However, *Tg(hand2:*EGFP) expression was not characterized during later stages of liver development.

The teleost zebrafish (*Danio rerio*) has emerged as a valuable vertebrate model system for studying liver development and disease. The zebrafish liver contains the same main cell types as the mammalian liver, including hepatocytes, biliary cells, and endothelial cells (13). Although the basic architecture of the fish liver differs from that of the mammalian liver, mechanisms of liver development and diseases are conserved (reviewed by 14). In addition, the zebrafish model presents important advantages that complement those of other animal models. The rapid external development and translucence of the embryos and larvae make them well suited for *in vivo* imaging analyses. Using transgenic approaches, investigators have generated zebrafish that express fluorescent proteins in different hepatic cell types, allowing easy visualization of hepatic cell behaviors in the animal, and greatly facilitating genetic and chemical screens to identify regulators of liver development and disease pathogenesis (reviewed by 14). Although intensive studies have been conducted on parenchymal cells in the zebrafish liver, no report has yet focused on HSCs.

In this study, we report that the *Tg(hand2:EGFP)* line marks HSCs during both embryonic and adult stages. Zebrafish HSCs share significant similarities with mammalian HSCs, including their morphology, localization, lipid storage, and gene expression. They respond to acute alcohol exposure by changing morphology, upregulating extracellular matrix protein production and increasing proliferation. By tracking HSCs throughout development, we show that zebrafish HSCs enter the liver after SECs do. Study of *cloche/clo* mutants

which lack SECs indicates that although SECs are not required for HSC differentiation or their entry into the liver, they influence the localization of HSCs inside the liver. We also reveal that inhibition of vascular endothelial growth factor (VEGF) signaling impairs entry of HSCs into the developing liver. Taken together, our work presents a new *in vivo* model to study HSC biology and provides novel insights into the molecular and cellular mechanisms underlying HSC development.

Materials and Methods

Zebrafish strains

Wild-type, clo$^{s5+/-}$, Tg(hand2:EGFP)^{pd24}, Tg(kdrl:ras-mCherry)^{s896}, Tg(fabp10a:dsRed)^{gz15} strains were maintained as described (15). The genotype of *clo*$^{s5-/-}$ embryos was determined by the lack of blood cells and severe edema (16). The University of California at San Francisco Institutional Animal Care and Use Committee approved all protocols.

Immunohistochemistry, in situ hybridization and gold chloride staining

Methods for these experiments are described in the Supporting Information.

Acute ethanol treatment and EdU cell cycle analysis

Acute ethanol treatment was conducted as described (17). To monitor the behaviors of HSCs after ethanol treatment, larvae were transferred back to embryo medium immediately after treatment and put on regular hatch fry diet.

To assess HSC proliferation during ethanol treatment, *Tg(hand2:EGFP)* larvae were incubated in 7 μM 5-ethynyl-2'deoxyuridine (EdU) dissolved in embryo medium with or without 2% ethanol for 24 hours. To assess HSC proliferation after treatment, control and ethanol-treated larvae were removed from ethanol and incubated in EdU solution for 24 hours. Animals were processed using the Click-iT EdU Imaging Kit (Invitrogen).

SU5416 treatment and microinjection of antisense morpholino oligonucleotide

Tg(hand2:EGFP;kdrl:ras-mCherry) animals were treated with 1 or 2 μM SU5416 (Sigma) in embryo medium at the stages indicated. Control animals from the same batch were treated with equal concentrations of DMSO. Microinjection of *kdrl* morpholino was performed as described (18). To quantify the number of intrahepatic vascular branches, three-dimensional projections were obtained from confocal stacks scanning through the entire liver. Each vascular branch was outlined using the Paintbrush tool in ImageJ and the number of branches was counted. For HSCs, the number of *Tg(hand2:*EGFP)-expressing cells located inside the liver was counted. Those cells that were still closely associated with the liver periphery were excluded. Statistical analyses were performed using the Student's two-tailed *t* test.

Gene-profiling analyses, quantitative real-time PCR and chemical screen

Materials and methods for these experiments are described in the Supporting Information.

Results

Tg(hand2:EGFP) expression marks HSCs in zebrafish

Consistent with the expression of endogenous *hand2* mRNA (Fig. 1A) (11), *Tg(hand2:*EGFP) is expressed in the neural crest and the lateral plate mesoderm and their derivatives during development (Fig. 1A'). Interestingly, we detected sparse expression of *Tg(hand2:*EGFP) within the liver. To determine the identity of these *Tg(hand2:*EGFP)-

expressing cells, we examined their morphology and distribution using confocal microscopy. By 4 days post fertilization (dpf), *Tg(hand2:*EGFP) is expressed in two distinct cell populations associated with the liver (Fig. 1B): one population forms a single cell layer lining the liver surface (arrows), whereas the other is located within the liver (asterisks). The cells inside the liver do not express molecular markers of hepatocytes (*Tg(fabp10a*:dsRed)) (19) (Fig. 1C), biliary cells (Alcam) (13) (Fig. 1D), or endothelial cells (*Tg(kdrl:ras*-mCherry)) (20) (Fig. 1E). They display a star-like configuration and form complex cellular processes that appear to wrap around endothelial cells (Fig 1E, arrows), features that are characteristic of HSCs (1). We also detected *Tg(hand2:*EGFP)-expressing cells in the adult liver where they exhibit similar morphology and close association with SECs (Fig. 1F).

To determine whether the *Tg(hand2:*EGFP)-expressing cells are indeed HSCs, we stained the animals with antibodies that recognize the HSC markers GFAP (3) (Fig. 2A, A') and desmin (4) (Fig. 2B, B'). At 128 hours post fertilization (hpf), we detected on average 55 *Tg(hand2:*EGFP)-expressing cells in the liver (8 embryos analyzed). 90% of these cells were labeled by the desmin antibody and 84% of them by the GFAP antibody. Thus *Tg(hand2:*EGFP) expression largely overlaps with HSC marker labeling. In mammals, HSCs serve as the main vitamin A-storing cells in the body. We performed gold chloride staining that labels retinoids (21) and found that the adult zebrafish liver stores vitamin A droplets (Fig. 2C). We also detected lipid droplets inside the *Tg(hand2:*EGFP)-expressing cells by Oil Red O staining (22) (Fig. 2D, asterisks). These data strongly suggest that *Tg(hand2:*EGFP) expression marks HSCs in zebrafish.

We isolated *Tg(hand2:*EGFP)-expressing cells from adult zebrafish livers via fluorescence-activated cell sorting (FACS), and performed gene-profiling analysis to detect transcripts that exhibit high expression levels in HSCs, but baseline expression levels in other hepatic cells (Supporting Fig. S1A). Among the most differentially expressed transcripts, we identified genes that have been previously implicated in mammalian HSC biology (Table S1; Supporting Fig. S1B-C). Hence, zebrafish HSCs exhibit a similar gene expression profile as their mammalian counterparts.

Zebrafish HSCs exhibit robust cellular responses to acute alcohol exposure

To determine the functional relevance between zebrafish and mammalian HSCs, we assessed the response of zebrafish cells to a hepatic insult. We selected ethanol as a stimulus, because alcoholic liver disease is an important cause of HSC activation and liver fibrosis (23), and because zebrafish represent an excellent model for studying the effects of alcohol on the liver (17). We exposed *Tg(hand2:EGFP)* larvae to 2% ethanol from 96 to 120 hpf and monitored the behaviors of HSCs during and after treatment. All the animals survived acute ethanol exposure but showed body abnormalities and erratic swimming behaviors (300 larvae from six clutches were examined). 60% of the treated animals developed steatosis, consistent with a previous report (17). We examined the deposition of matrix proteins in untreated control and ethanol-treated livers. Whereas laminin was almost undetectable in control livers (Fig. 3A'), its deposition was markedly elevated in ethanol-treated livers (Fig. 3B'), suggesting that acute ethanol exposure stimulates matrix deposition by zebrafish HSCs. Similar to laminin, type IV collagen was also deposited in excess in ethanol-treated livers (data not shown). Furthermore, the morphology of HSCs was altered after ethanol treatment: they lost the complex cytoplasmic processes and their cell bodies became more elongated (Fig. 3B).

When ethanol-treated animals were transferred back to embryo medium, their body phenotypes and abnormal swimming behaviors recovered within a day and more than 70% of the animals survived for at least one week. During the followup period after ethanol removal, HSCs rapidly increased in number in ethanol-treated animals compared to controls

(Fig. 3C-E). To determine whether cell proliferation contributed to this increase in HSC number, we examined incorporation of the proliferation marker EdU by these cells. In untreated animals, 20% of the HSCs showed EdU incorporation and this percentage was unchanged during ethanol treatment (Fig. 3F). However, one day after treatment, approximately 40% of the HSCs in ethanol-treated larvae incorporated EdU, compared to 28% in controls (Fig. 3F). Thus HSCs became more proliferative after acute ethanol treatment, which was at least partially responsible for the increase in HSC cell number in treated livers.

Taken together, our observations indicate that zebrafish HSCs exhibit enhanced matrix protein deposition, morphological changes, and increased proliferation upon acute alcohol exposure. They support the concept that zebrafish HSCs are functionally similar to their mammalian counterparts during liver injury.

HSC development in zebrafish

The process of HSC development is incompletely understood. The close association between HSCs and SECs suggests that SECs may play a role in HSC development. We performed time course analyses to monitor the interactions between HSCs and SECs during development. To visualize SECs, we used the *Tg(kdrl:ras-mCherry)* line, in which the promoter of the VEGF-receptor gene *kdrl* drives ras-mCherry expression (20). We detected strong *Tg(kdrl:*ras-mCherry) expression in SECs but not in HSCs, enabling us to distinguish between these two cell populations in *Tg(hand2:EGFP;kdrl:ras-mCherry)* animals.

Early zebrafish liver development proceeds without SECs, which do not enter the liver prior to 55 hpf (13). Between 62 and 64 hpf, SECs are situated mostly at the dorsal surface of the liver (Fig. 4A, B, arrows), while *Tg(hand2:*EGFP)-expressing cells are restricted to the boundary between the liver and the gut (Fig. 4A, B, asterisks). By 66 hpf, SECs begin to invade the liver (Fig. 4C, arrow) (13), while *Tg(hand2:*EGFP)-expressing cells remain at the liver periphery (Fig. 4C, asterisks). From 68 hpf onwards, HSCs gradually spread throughout the liver (Fig. 4D-F). Both HSCs and SECs seem to enter the liver at random locations. Whereas some SECs invade the liver without being accompanied by HSCs (Fig. 4D, arrow), all HSCs maintain close proximity to SECs once they are inside the liver (Fig. 4D, arrowheads).

While tracking HSC development, we noticed that the number of HSCs increased from 5±4 to 33±10 (average±standard deviation) between 65 and 81 hpf. To determine whether proliferation of HSCs accounted for the increase in HSC number, we performed immunohistochemistry with the anti-Phospho-histone 3 antibody to label M-phase cells (24) (Fig. 4G-J). In all the animals examined, we detected 100 Phospho-histone 3 and *Tg(hand2:*EGFP) double positive cells in the liver. However, only eight of these cells resided inside the liver (Fig. 4G, arrow), while the remainder were located at the liver periphery (Fig. 4H-J, arrows). These results suggest that *Tg(hand2:*EGFP)-expressing cells proliferate mainly at the liver periphery prior to entering the liver.

SECs influence the localization of HSCs in the developing liver

To investigate the role of SECs in HSC development, we examined *Tg(hand2:*EGFP) expression in embryos homozygous for the *clo* mutation, which lack most hematopoietic and endothelial cells (16). At 4 dpf, whereas wild-type livers formed a rudimentary intrahepatic vascular network as revealed by *Tg(kdrl:*ras-mCherry) expression (Fig. 5A, A'), we did not detect any *Tg(kdrl:*ras-mCherry) expression in *clo* mutant livers (Fig. 5B, B'). It has been shown that in zebrafish, endothelial cells are not required for liver budding or hepatocyte differentiation (25), but they appear to be essential for further growth of the liver (26).

Consistent with these reports, *clo* mutant livers contained only two-thirds as many Prox1+ parenchymal cells as wild-type livers at 4 dpf (Fig. 5E). However, the number of *Tg(hand2:*EGFP)-expressing cells inside the liver was similar in wild-type and mutants (Fig. 5E), providing direct evidence that HSCs do not derive from endothelial cells and that they do not rely on SECs to enter the liver.

In mammals, HSCs are situated in the space of Disse, which sits beneath the basolateral surface of hepatocytes, whereas biliary cells are restricted to the portal regions (reviewed by 27). We found that in wild-type zebrafish livers, the cell bodies of HSCs are separated from biliary cells by hepatocytes (Fig. 5C). Strikingly, in *clo* mutant livers, HSCs appear to be closely associated with biliary cells (Fig. 5D, arrows), suggesting that loss of SECs alters the relationships amongst HSCs, hepatocytes and biliary cells.

Inhibition of VEGF signaling leads to a decrease in HSC number

The angiogenic factor VEGF and its receptors are induced in activated HSCs during liver injury, and VEGF signaling has been shown to mediate the cross talk between SECs and HSCs (reviewed by 1). To determine whether VEGF is also involved in SEC-HSC interactions during development, we treated *Tg(hand2:EGFP;kdrl:ras-mCherry)* animals with SU5416, a potent and selective inhibitor of the Flk-1/KDR receptor tyrosine kinase (28). SU5416 has been shown to effectively block VEGF signaling and angiogenesis in zebrafish (29, 30). In agreement with these reports, we observed a dose-dependent decrease in the number of intrahepatic vascular branches in animals treated with SU5416 between 55 and 80 hpf (Fig. 6A-B). The number of HSCs was significantly reduced upon SU5416 treatment (Fig. 6A, C), although most remaining HSCs still kept close contact with SECs (data not shown). When we treated animals with SU5416 between 72 and 96 hpf, after significant numbers of SECs and HSCs had entered the liver, we observed a much milder deficiency of SECs and HSCs (Fig. 6A-C).

To test the specific requirement of Kdrl in HSC and SEC development, we injected *Tg(hand2:EGFP; kdrl:ras-mCherry)* embryos with an antisense morpholino (MO) targeted against *kdrl* (18). Consistent with previous data (18), injection of 3 ng of *kdrl* MO resulted in a severe reduction of blood vessels (data not shown). We did not detect any *Tg(kdrl:*ras-mCherry*)* expression in the liver in *kdrl*-knock down animals (Fig. 6D). Similar to the phenotypes caused by SU5416 treatment, we observed a significant reduction of HSCs in *kdrl*-knock down animals (Fig. 6D). Such a reduction was not likely due to a delay in liver growth as the numbers of Prox1+ parenchymal cells were similar between uninjected controls and *kdrl*-knock down animals ($p>0.11$, 10 control and 10 *kdrl*-knock down animals were analyzed).

The modulation of VEGF signaling may directly affect both SECs and HSCs. However, it is also possible that SECs are primarily affected, with the ensuing decrease in HSCs resulting from alterations in signaling between SECs and HSCs. If the latter scenario was correct, inhibition of VEGF signaling should not affect HSCs in the absence of SECs. We therefore conducted SU5416 treatments on *clo* mutants and found that they caused a dose- and stage-dependent decrease in HSC cell number similar to the decrease seen in wild-type (Fig. 6E). This result indicates that inhibition of VEGF signaling independently impairs both HSCs and SECs.

Retinoid receptor agonists alter HSC numbers

The identification of bioactive compounds that affect HSC behavior could provide insight into HSC biology and offer means to manipulate HSCs during liver injury or disease. We performed a pilot screen of 338 compounds, looking for agents that caused either a decrease

or an increase in HSC numbers. Animals were treated with compounds from 55 to 80 hpf (Fig. 7A; Supporting Information). We found that AM580, a retinoic acid receptor (RAR)-alpha-selective agonist (31), decreased HSC numbers (Fig. 7B-C). By contrast, methoprene acid (MA), a retinoid X receptor (RXR) agonist (32), increased the numbers of HSCs (Fig. 7B-C). Neither drug affected gross liver morphology or larval survival. These data indicate that retinoid receptor agonists alter HSC numbers *in vivo*, which is consistent with a previous report that retinoic acid signaling regulates HSC development (33). Furthermore, the identification of two HSC-altering compounds in our pilot screen validates this approach as a way to discover compounds that impact HSC biology.

Discussion

Here we present the first HSC reporter line in zebrafish, *Tg(hand2:EGFP)*. Similar to mammalian HSCs, zebrafish HSCs are in close proximity to SECs, exhibit stellate morphology and store lipid droplets. Importantly, they display robust cellular responses to acute ethanol exposure, and thus are functionally equivalent to their mammalian counterparts in response to this hepatic insult. We tracked the development of HSCs and show that they enter the liver after SECs do. By analyzing *clo* mutants, we reveal that SECs are not required for HSC differentiation or their entry into the liver. However, in the absence of SECs, HSCs associate instead with biliary cells. We also show that inhibition of VEGF signaling significantly reduces the number of HSCs that enter the liver, even in the absence of SECs. Lastly, we demonstrate the use of the HSC reporter line in gene-profiling analyses and chemical screens to identify novel molecular mechanisms underlying HSC development. Our study provides a detailed characterization of HSC development in zebrafish, and validates the usefulness of this model organism in HSC research.

The embryonic origin of HSCs is elusive due to their diverse gene expression. We show that in zebrafish, HSCs express *hand2* which labels mesodermal and neural crest derivatives and supports a mesodermal and neural crest origin for HSCs. It has been hypothesized that HSCs and SECs share a common precursor. Studies of HSC-SEC interactions have been limited, in part because mouse mutants deficient in endothelial cells exhibit early embryonic lethality (34). Unlike the mammalian liver, the zebrafish liver is not a hematopoietic organ and liver defects do not lead to anemia or early lethality (25). We detected HSCs in *clo* mutants which lack SECs, thereby providing direct evidence that HSCs do not originate from SECs or their precursors in zebrafish.

Our analyses of *clo* mutants reveal a surprising role for SECs in the localization of HSCs during liver development. In normal livers, SECs guide HSCs to their proper sinusoidal location. When SECs are absent, HSCs do not fail to migrate into the liver; instead, they become abnormally associated with biliary cells. It is possible that in normal livers, SECs and biliary cells both have the capacity to control HSC migration, with SECs being dominant. Alternatively, biliary cells may have no inherent ability to attract HSC in normal livers, but in the absence of SECs, may acquire a novel phenotype with this capacity. In biliary diseases, cholangiocytes are thought to undergo epithelial-to-mesenchymal transition (EMT), by which they acquire features of mesenchymal cells (reviewed by 35). It will be interesting to determine whether EMT of biliary cells contributes to the altered HSC distribution in *clo* mutants. Biliary-HSC interactions play important roles in biliary diseases, and paracrine signals including chemokines, cytokines, purinergic agonists, and morphogens such as Hedgehog have been shown to mediate these interactions (reviewed by 35). Further study of *clo* mutants may identify additional paracrine signals, thereby advancing our understanding of biliary-HSC interactions in normal and diseased livers.

We show that VEGF signaling inhibition via chemical inhibitor treatments or *kdrl* MO injections decreases HSC numbers and that this effect still occurs in the absence of SECs. VEGF signaling does not seem to be essential for differentiation and survival of HSCs, as blocking VEGF signaling during later stages only causes a mild decrease in HSC numbers. Rather, VEGF signaling may be required for the initial wave of HSCs entering the liver. During later development, when significant numbers of HSCs and SECs are present in the liver, different signals, possibly from the existing HSCs and SECs, might play a greater role in attracting additional HSCs. Meanwhile, because both of our approaches induced global inhibition of VEGF signaling, it is plausible that they also impair hepatocytes and/or biliary cells, which may contribute to the reduction in HSC numbers. In the future, it will be necessary to knock down VEGF receptor function selectively in HSCs to determine the HSC-specific requirement of VEGF signaling.

We describe a pilot chemical screen to identify drugs affecting HSC development. Chemical screens using zebrafish have several advantages over those performed in cultured cells (36, 37). First, the zebrafish system enables one to identify drugs that cause specific phenotypes in HSCs without causing substantial toxicity to other organs. Second, *in vivo* systems enable the identification of compounds that require the presence of additional cell types, matrix components and/or growth factors to help mediate their effects. Finally, drugs identified through *in vitro* screens may not be effective in live animals, perhaps because of critical differences in gene expression (37). Our pilot screen resulted in the identification of two retinoid receptor agonists, AM580 and MA, that caused opposite effects on HSC numbers. Although HSCs have a well-established role in retinoid storage and transport, the role of retinoids in regulating HSC proliferation and fibrogenesis is incompletely understood, and reports investigating the effects of retinoids on HSCs have been contradictory (reviewed by 1). Interestingly, all-*trans*-retinoic acid (RA), 9-*cis*-RA, and synthetic retinoids have divergent effects on activated HSCs in culture (38), supporting the hypothesis that RXR and RAR have at least some non-overlapping effects in HSCs. It will be interesting to further explore the role of retinoid signaling during development and injury using the *Tg(hand2:EGFP)* line, as well as to extend the chemical screen to identify additional compounds with effects on HSC biology.

Our work demonstrates that the *Tg(hand2:EGFP)* line represents a versatile *in vivo* model for HSC research that complements cell culture and mammalian systems. More importantly, it illustrates that this HSC reporter line can be applied not only to the study of HSC development, but also to the study of their activation in liver injury, as acute alcohol insult triggers robust cellular responses of zebrafish HSCs similar to those observed in activated HSCs in mammalian liver injury. The functional similarities between zebrafish and mammalian HSCs, combined with the unique strengths of the zebrafish model, open up numerous exciting new avenues for studying HSC biology in liver injury.

Supplementary Material

Refer to Web version on PubMed Central for supplementary material.

Acknowledgments

We would like to thank Drs. Scott Friedman and D. Montgomery Bissell for critical comments and support, and Stainier lab members for technical advice and discussions. We acknowledge the UCSF Liver Center for technical support and the UCSF Genomics Core Facility for conducting quantitative real-time PCR. We thank Sarah Elmes for assistance with FACS and Ana Ayala, Milagritos Alva and Mark Sklar for fish care.

Financial support:

Chunyue Yin is supported by Grant Number K99AA020514 from the NIH, and the UCSF Liver Center Pilot/Feasibility Award (NIH P30DK026743); Kimberley J. Evason is a Damon Runyon Fellow supported by the Damon Runyon Cancer Research Foundation (DRG-109-10); Jacquelyn J. Maher is supported by grants from the NIH (R01DK068450, R01DK088674, and P30DK026743); this work was supported in part by grants from the NIH (R01DK060322) and the Packard Foundation to Didier Y. R. Stainier.

Abbreviations

HSC	hepatic stellate cell
SEC	sinusoidal endothelial cell
Wt1	Wilms' tumor suppressor gene
GFAP	glial fibrillary acidic protein
hand2	heart and neural crest derivatives expressed transcript 2
clo	cloche
VEGF	vascular endothelial cell growth factor
dpf	days post fertilization
hpf	hours post fertilization
FACS	fluorescence-activated cell sorting
MO	morpholino
MA	methoprene acid
RAR	retinoic acid receptor
RXR	retinoid X receptor
EMT	epithelial-to-mesenchymal transition
RA	retinoic acid
A	anterior
P	posterior
L	left
R	right
D	dorsal
V	ventral
Int	intestine
Li	liver
Ph	pharyngeal arch
Fin	fin bud
Prox1	Prospero-related homeobox gene 1
EtOH	ethanol
dpt	days post treatment

References

1. Friedman SL. Hepatic stellate cells: protean, multifunctional, and enigmatic cells of the liver. Physiol Rev. 2008; 88:125–172. [PubMed: 18195085]

2. Atzori L, Poli G, Perra A. Hepatic stellate cell: a star cell in the liver. Int J Biochem Cell Biol. 2009; 41:1639–1642. [PubMed: 19433304]
3. Gard AL, White FP, Dutton GR. Extra-neural glial fibrillary acidic protein (GFAP) immunoreactivity in perisinusoidal stellate cells of rat liver. J Neuroimmunol. 1985; 8:359–375. [PubMed: 3891783]
4. Yokoi Y, Namihisa T, Kuroda H, Komatsu I, Miyazaki A, Watanabe S, Usui K. Immunocytochemical detection of desmin in fat-storing cells (Ito cells). Hepatology. 1984; 4:709–714. [PubMed: 6204917]
5. Asahina K, Zhou B, Pu WT, Tsukamoto H. Septum transversum-derived mesothelium gives rise to hepatic stellate cells and perivascular mesenchymal cells in developing mouse liver. Hepatology. 2011; 53:983–995. [PubMed: 21294146]
6. Perez-Pomares JM, Carmona R, Gonzalez-Iriarte M, Macias D, Guadix JA, Munoz-Chapuli R. Contribution of mesothelium-derived cells to liver sinusoids in avian embryos. Dev Dyn. 2004; 229:465–474. [PubMed: 14991702]
7. Ankoma-Sey V, Matli M, Chang KB, Lalazar A, Donner DB, Wong L, Warren RS, et al. Coordinated induction of VEGF receptors in mesenchymal cell types during rat hepatic wound healing. Oncogene. 1998; 17:115–121. [PubMed: 9671320]
8. Magness ST, Bataller R, Yang L, Brenner DA. A dual reporter gene transgenic mouse demonstrates heterogeneity in hepatic fibrogenic cell populations. Hepatology. 2004; 40:1151–1159. [PubMed: 15389867]
9. Winau F, Hegasy G, Weiskirchen R, Weber S, Cassan C, Sieling PA, Modlin RL, et al. Ito cells are liver-resident antigen-presenting cells for activating T cell responses. Immunity. 2007; 26:117–129. [PubMed: 17239632]
10. Yang L, Jung Y, Omenetti A, Witek RP, Choi S, Vandongen HM, Huang J, et al. Fate-mapping evidence that hepatic stellate cells are epithelial progenitors in adult mouse livers. Stem Cells. 2008; 26:2104–2113. [PubMed: 18511600]
11. Angelo S, Lohr J, Lee KH, Ticho BS, Breitbart RE, Hill S, Yost HJ, et al. Conservation of sequence and expression of Xenopus and zebrafish dHAND during cardiac, branchial arch and lateral mesoderm development. Mech Dev. 2000; 95:231–237. [PubMed: 10906469]
12. Yin C, Kikuchi K, Hochgreb T, Poss KD, Stainier DY. Hand2 regulates extracellular matrix remodeling essential for gut-looping morphogenesis in zebrafish. Dev Cell. 2010; 18:973–984. [PubMed: 20627079]
13. Sakaguchi TF, Sadler KC, Crosnier C, Stainier DY. Endothelial signals modulate hepatocyte apicobasal polarization in zebrafish. Curr Biol. 2008; 18:1565–1571. [PubMed: 18951027]
14. Chu J, Sadler KC. New school in liver development: lessons from zebrafish. Hepatology. 2009; 50:1656–1663. [PubMed: 19693947]
15. Kimmel CB, Ballard WW, Kimmel SR, Ullmann B, Schilling TF. Stages of embryonic development of the zebrafish. Dev Dyn. 1995; 203:253–310. [PubMed: 8589427]
16. Stainier DY, Weinstein BM, Detrich HW 3rd, Zon LI, Fishman MC. Cloche, an early acting zebrafish gene, is required by both the endothelial and hematopoietic lineages. Development. 1995; 121:3141–3150. [PubMed: 7588049]
17. Passeri MJ, Cinaroglu A, Gao C, Sadler KC. Hepatic steatosis in response to acute alcohol exposure in zebrafish requires sterol regulatory element binding protein activation. Hepatology. 2009; 49:443–452. [PubMed: 19127516]
18. Habeck H, Odenthal J, Walderich B, Maischein H, Schulte-Merker S. Analysis of a zebrafish VEGF receptor mutant reveals specific disruption of angiogenesis. Curr Biol. 2002; 12:1405–1412. [PubMed: 12194822]
19. Her GM, Chiang CC, Chen WY, Wu JL. In vivo studies of liver-type fatty acid binding protein (L-FABP) gene expression in liver of transgenic zebrafish (Danio rerio). FEBS Lett. 2003; 538:125–133. [PubMed: 12633865]
20. Chi NC, Shaw RM, De Val S, Kang G, Jan LY, Black BL, Stainier DY. Foxn4 directly regulates tbx2b expression and atrioventricular canal formation. Genes Dev. 2008; 22:734–739. [PubMed: 18347092]

21. Wake K, Motomatsu K, Senoo H, Masuda A, Adachi E. Improved Kupffer's gold chloride method for demonstrating the stellate cells storing retinol (vitamin A) in the liver and extrahepatic organs of vertebrates. Stain Technol. 1986; 61:193–200. [PubMed: 2428130]
22. Koopman R, Schaart G, Hesselink MK. Optimisation of oil red O staining permits combination with immunofluorescence and automated quantification of lipids. Histochem Cell Biol. 2001; 116:63–68. [PubMed: 11479724]
23. Friedman SL. Stellate cell activation in alcoholic fibrosis--an overview. Alcohol Clin Exp Res. 1999; 23:904–910. [PubMed: 10371412]
24. Ajiro K, Yoda K, Utsumi K, Nishikawa Y. Alteration of cell cycle-dependent histone phosphorylations by okadaic acid. Induction of mitosis-specific H3 phosphorylation and chromatin condensation in mammalian interphase cells. J Biol Chem. 1996; 271:13197–13201. [PubMed: 8662672]
25. Field HA, Ober EA, Roeser T, Stainier DY. Formation of the digestive system in zebrafish. I. Liver morphogenesis. Dev Biol. 2003; 253:279–290. [PubMed: 12645931]
26. Korzh S, Pan X, Garcia-Lecea M, Winata CL, Wohland T, Korzh V, Gong Z. Requirement of vasculogenesis and blood circulation in late stages of liver growth in zebrafish. BMC Dev Biol. 2008; 8:84. [PubMed: 18796162]
27. Si-Tayeb K, Lemaigre FP, Duncan SA. Organogenesis and development of the liver. Dev Cell. 2010; 18:175–189. [PubMed: 20159590]
28. Fong TA, Shawver LK, Sun L, Tang C, App H, Powell TJ, Kim YH, et al. SU5416 is a potent and selective inhibitor of the vascular endothelial growth factor receptor (Flk-1/KDR) that inhibits tyrosine kinase catalysis, tumor vascularization, and growth of multiple tumor types. Cancer Res. 1999; 59:99–106. [PubMed: 9892193]
29. Serbedzija GN, Flynn E, Willett CE. Zebrafish angiogenesis: a new model for drug screening. Angiogenesis. 1999; 3:353–359. [PubMed: 14517415]
30. Cross LM, Cook MA, Lin S, Chen JN, Rubinstein AL. Rapid analysis of angiogenesis drugs in a live fluorescent zebrafish assay. Arterioscler Thromb Vasc Biol. 2003; 23:911–912. [PubMed: 12740225]
31. Gianni M, Li Calzi M, Terao M, Guiso G, Caccia S, Barbui T, Rambaldi A, et al. AM580, a stable benzoic derivative of retinoic acid, has powerful and selective cyto-differentiating effects on acute promyelocytic leukemia cells. Blood. 1996; 87:1520–1531. [PubMed: 8608243]
32. Harmon MA, Boehm MF, Heyman RA, Mangelsdorf DJ. Activation of mammalian retinoid X receptors by the insect growth regulator methoprene. Proc Natl Acad Sci U S A. 1995; 92:6157–6160. [PubMed: 7597096]
33. Ijpenberg A, Perez-Pomares JM, Guadix JA, Carmona R, Portillo-Sanchez V, Macias D, Hohenstein P, et al. Wt1 and retinoic acid signaling are essential for stellate cell development and liver morphogenesis. Dev Biol. 2007; 312:157–170. [PubMed: 18028902]
34. Matsumoto K, Yoshitomi H, Rossant J, Zaret KS. Liver organogenesis promoted by endothelial cells prior to vascular function. Science. 2001; 294:559–563. [PubMed: 11577199]
35. Fabris L, Strazzabosco M. Epithelial-mesenchymal interactions in biliary diseases. Semin Liver Dis. 2011; 31:11–32. [PubMed: 21344348]
36. Lee MK, Ha NR, Yang H, Sung SH, Kim GH, Kim YC. Antiproliferative activity of triterpenoids from Eclipta prostrata on hepatic stellate cells. Phytomedicine. 2008; 15:775–780. [PubMed: 18061418]
37. Marek CJ, Wallace K, Durward E, Koruth M, Leel V, Leiper LJ, Wright MC. Low affinity glucocorticoid binding site ligands as potential anti-fibrogenics. Comp Hepatol. 2009; 8:1. [PubMed: 19432992]
38. Hellemans K, Verbuyst P, Quartier E, Schuit F, Rombouts K, Chandraratna RA, Schuppan D, et al. Differential modulation of rat hepatic stellate phenotype by natural and synthetic retinoids. Hepatology. 2004; 39:97–108. [PubMed: 14752828]

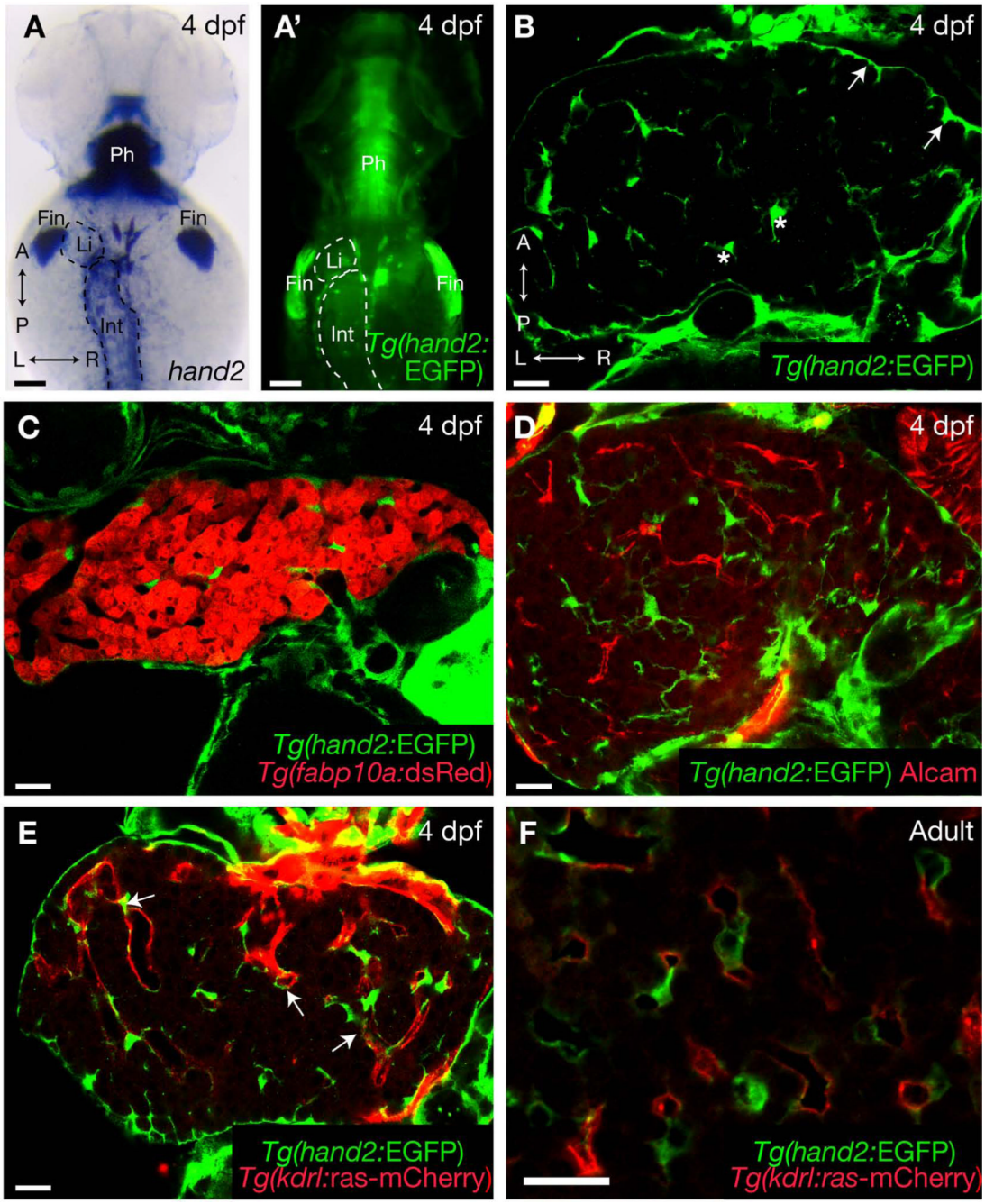

Fig. 1.

*Tg(hand2:*EGFP) is expressed in a novel cell population within the zebrafish liver. (A) Whole-mount *in situ* hybridization shows the endogenous expression of *hand2* in wild-type larvae at 4 days post fertilization (dpf). *hand2* is expressed in the pharyngeal arch (Ph), fin bud (Fin), liver (Li), and the mesenchyme surrounding the intestine (Int). (A') *Tg(hand2:*EGFP) expression resembles the endogenous expression of *hand2*. (B) At 4 dpf, *Tg(hand2:*EGFP) is expressed in a single-celled layer (arrows) lining the liver , as well as in star-shaped cells inside the liver (asterisks). (C-E) Expression of *Tg(hand2:*EGFP) does not overlap with the expression of the hepatocyte marker *Tg(fabp10a:*dsRed) (C), the biliary cell marker Alcam (D), or the endothelial cell marker *Tg(kdrl:*ras-mCherry) (E). Notably,

*Tg(hand2:*EGFP)-expressing cells appear to wrap around endothelial cells (E, arrows). (F) *Tg(hand2:*EGFP) expression in a vibratome section of adult zebrafish liver. Similar to what is observed in the larval liver, *Tg(hand2:*EGFP)-expressing cells in the adult liver reside in close proximity to endothelial cells. (A, A') Whole-mount zebrafish larvae, dorsal views, anterior to the top. (B-F) Confocal single-plane images of zebrafish livers. (B-E) Dorsal views, anterior to the top. A, anterior; P, posterior; L, left; R, right. Scale bars: (A, A') 100 μm; (B-F) 20 μm.

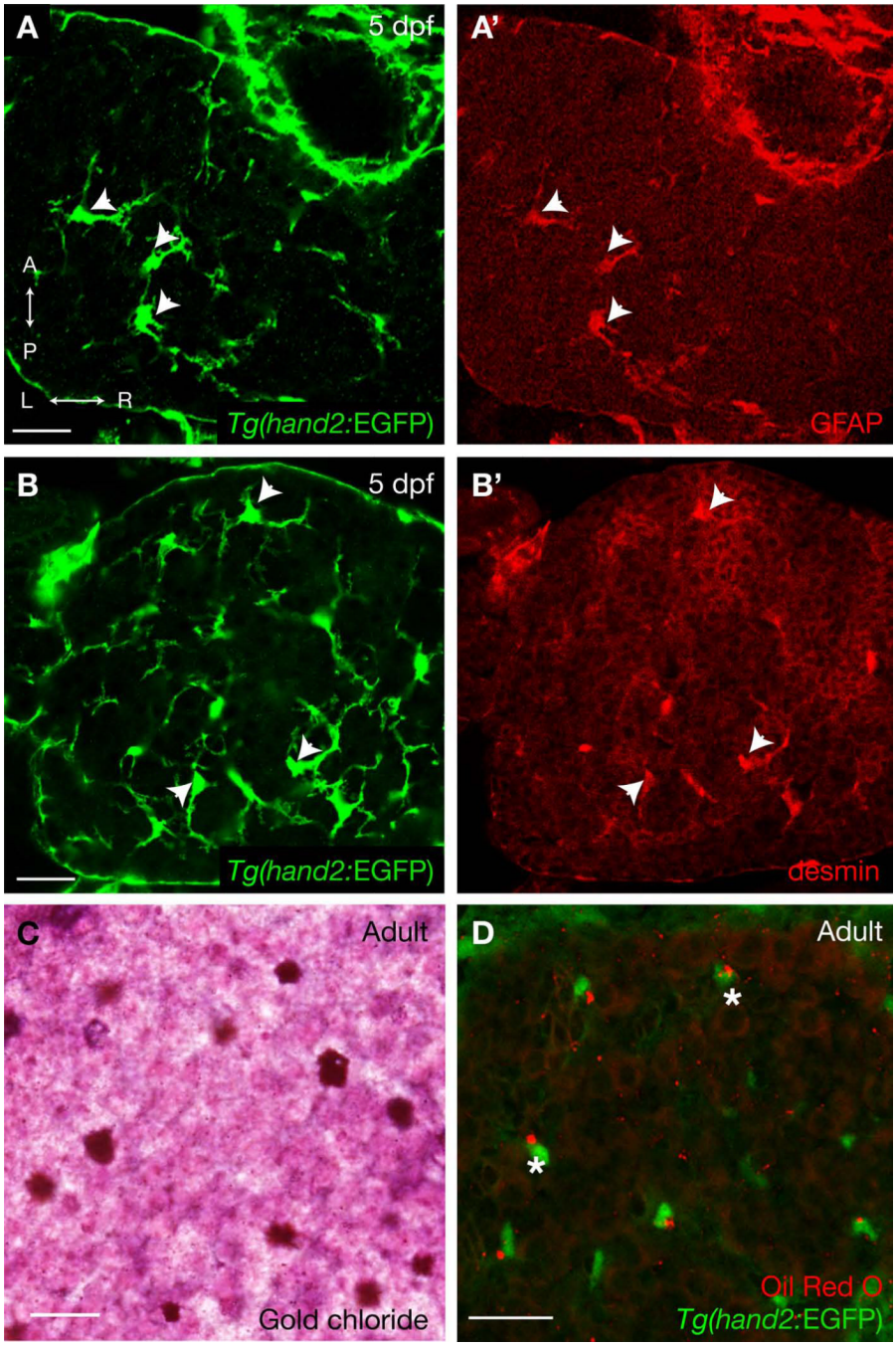

Fig. 2.

*Tg(hand2:*EGFP) expression marks HSCs in the zebrafish liver. (A-B) *Tg(hand2:*EGFP) expression in the liver at 5 dpf. (A'-B') Same views as (A-B), but showing immunostaining for GFAP and desmin. *Tg(hand2:*EGFP) expression largely overlaps with GFAP and desmin antibody labeling at this stage (arrowheads). (C) Vibratome section of adult zebrafish liver shows the presence of vitamin A as revealed by gold chloride staining. (D) *Tg(hand2:*EGFP)-expressing cells deposit lipid droplets as shown by Oil Red O staining on a vibratome section of adult liver. (A-B, A'-B', D) Confocal single-plane images of the zebrafish liver. (A-B, A'-B') Dorsal views, anterior to the top. Scale bars, 20 μm.

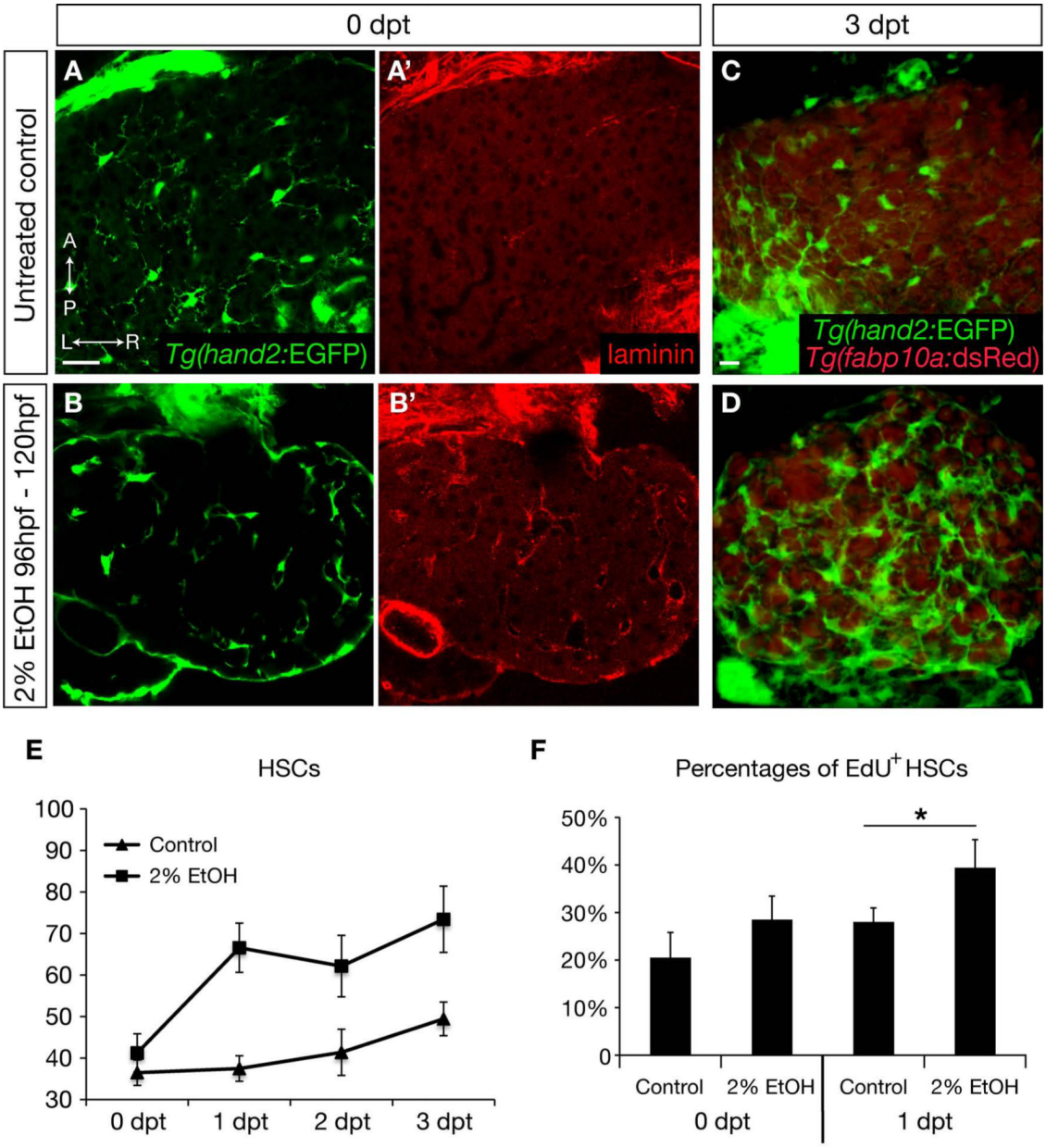

Fig. 3.

Acute ethanol treatment leads to increased deposition of extracellular matrix proteins and HSC number. (A, B) Confocal single-plane images of HSCs in untreated controls (A) and larvae treated with 2% ethanol from 96 to 120 hpf (B). Animals were collected and examined immediately after treatment. (A', B') same views as (A, B), but showing the deposition of laminin. HSCs in ethanol-treated animals upregulated their production of laminin and exhibited changes in morphology. 30 control and 30 ethanol-treated animals from six clutches were examined and all showed an increase in laminin deposition. (C, D) Confocal projections showing HSCs in untreated controls and ethanol-treated larvae at three days post treatment (dpt). HSCs in ethanol-treated larvae are more numerous, and show more elongated cell bodies and less complex cytoplasmic processes. (E) Numbers (mean ±SEM) of HSCs in control and ethanol-treated animals immediately after treatment (0 dpt), and at 1, 2, and 3 days post treatment. At each time point, 10 control and 10 ethanol-treated

larvae from two clutches were examined. The differences in HSC cell number between control and treated animals at 1, 2, and 3 dpt were statistically significant ($p<0.05$). (F) Percentages (mean ±SEM) of HSCs that had incorporated EdU during or at one day after ethanol treatment. At both time points, 10 control and 10 ethanol-treated larvae were examined. Asterisk indicates statistical significance: *$p<0.05$. (A-D) Dorsal views, anterior to the top. Scale bars, 20 μm.

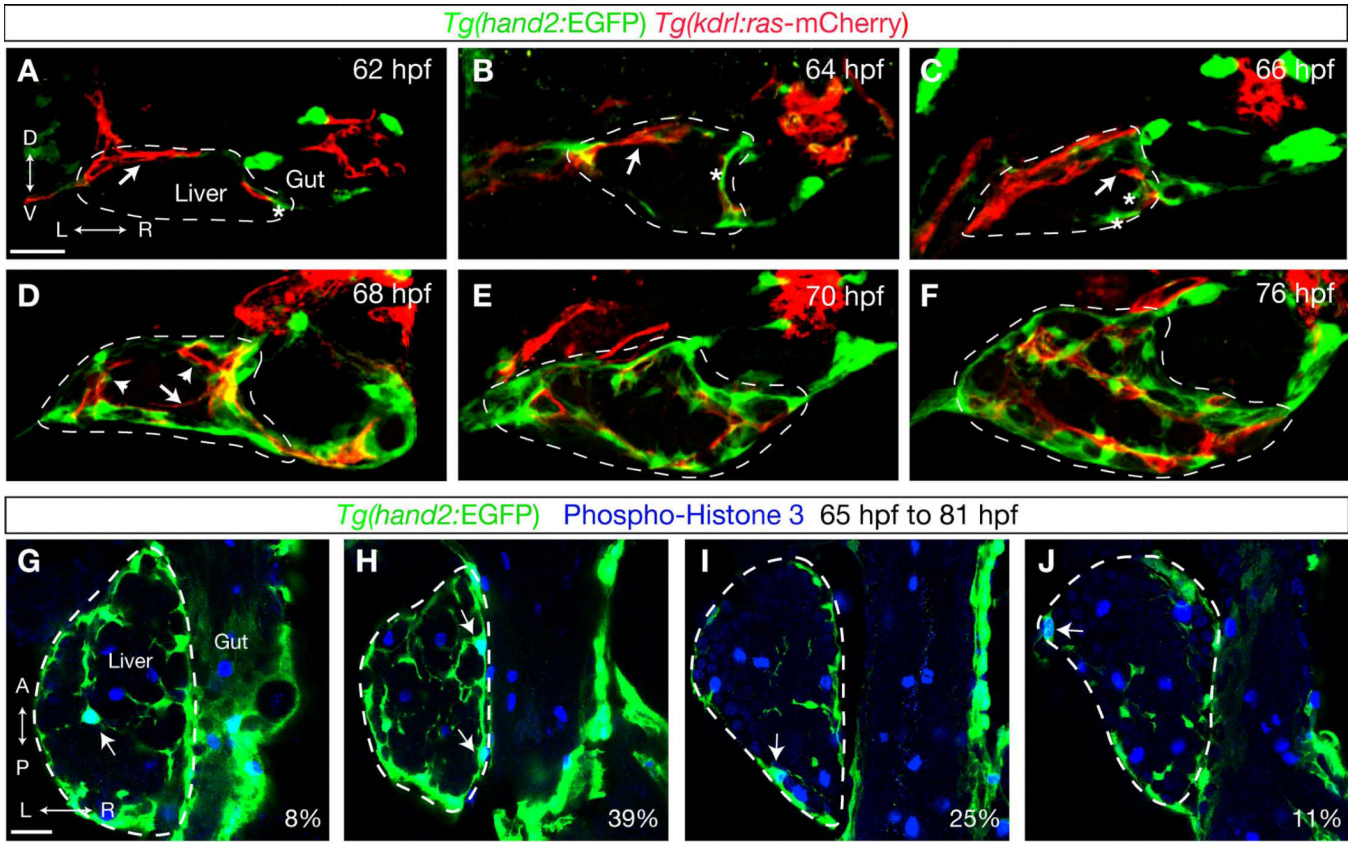

Fig. 4.

HSC development in zebrafish. (A-F) Time course analysis of HSCs and SECs in *Tg(hand2:EGFP; kdrl:ras-mCherry)* larvae. Eight larvae were fixed every two hours between 62 and 76 hpf, and stained for GFP (green) and dsRed (red). Arrows and asterisks in (A-B) mark the positions of SECs and HSCs, respectively. Arrows in (C-D) point to SECs that have entered the liver without being accompanied by HSCs. Arrowheads in (D) point to HSCs that have entered the liver in association with SECs. (A-F) Confocal projections of transverse vibratome sections, dorsal to the top. (G-H) HSCs inside the liver exhibited low proliferation rates. Five *Tg(hand2:EGFP)* larvae were fixed every two hours between 65 and 81 hpf and stained for Phospho-histone 3 (blue) which labels proliferating cells. 100 *Tg(hand2:*EGFP)-expressing cells were found to be Phospho-histone 3 positive, but only eight of them were located inside the liver (arrow in G). The remaining cells were located at the periphery of the liver (arrows in H-J). Among these cells, 39 of them were located proximal to the gut (arrows in H), 25 were located posteriorly (arrow in I), and 11 were located distal to the gut (arrow in J). (G-J) Confocal single-plane images of the liver, anterior to the top. (A-J) Dashed lines outline the liver. Scale bars, 20 μm. D, dorsal; V, ventral.

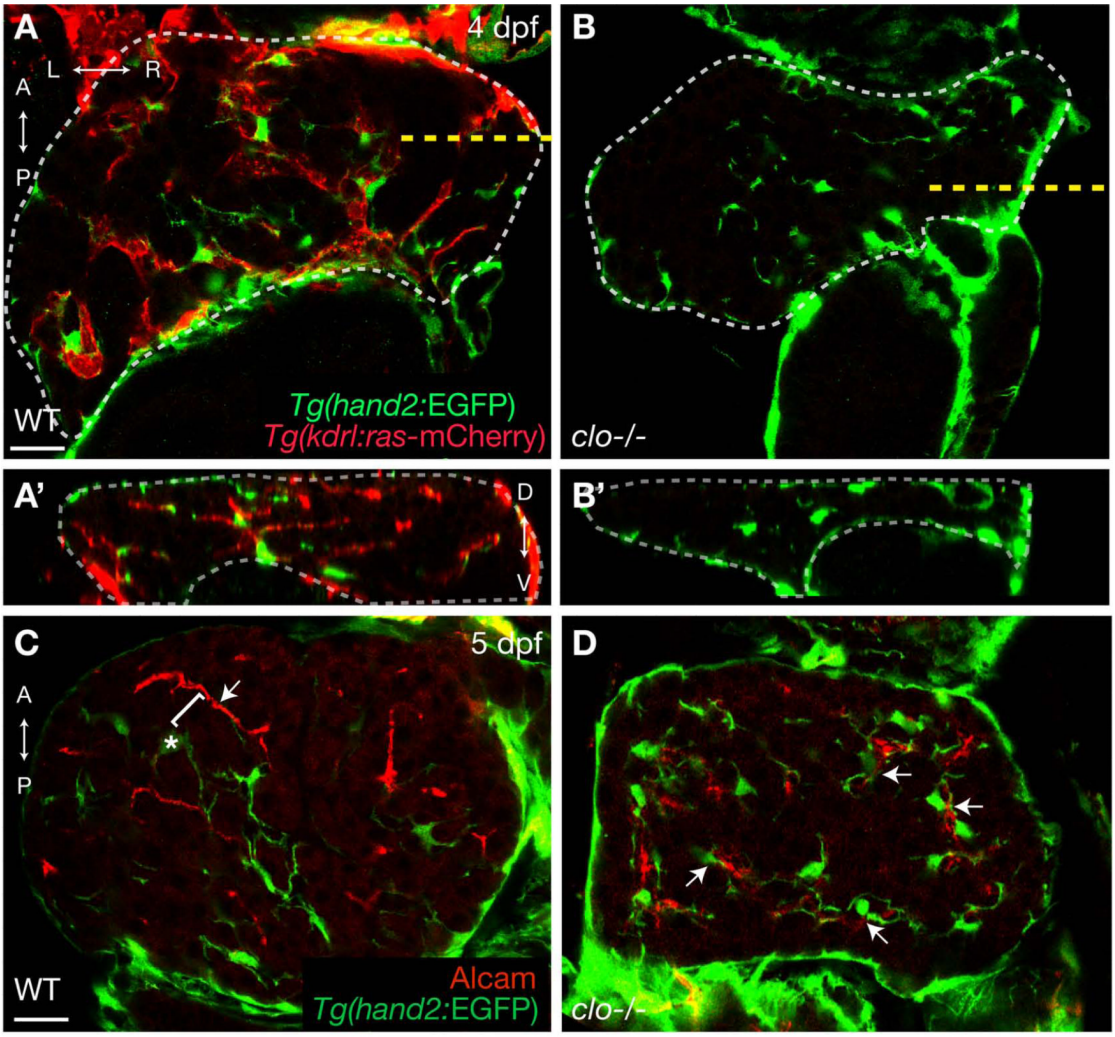

E

	WT	*clo*-/-	*p*-value
Hepatocytes per larva	1508 ± 123	951 ± 89	0.0107 *
HSCs per larva	31 ± 4	34 ± 2	0.5132
HSCs/Hepatocytes	0.020 ± 0.002	0.037 ± 0.001	0.0003 ***

Fig. 5.

clo mutant livers still contain *Tg(hand2:*EGFP)-expressing cells . (A-B) Wild-type and *clo* mutant larvae were collected from an incross of *clo* heterozygous fish that were also homozygous for the *hand2:EGFP* and *kdrl:ras-mCherry* transgenes. By 4 dpf, whereas wild-type livers formed a clear vascular network as revealed by *Tg(kdrl:*ras-mCherry) expression (A), endothelial cells were completely missing in *clo* mutant livers (B). (A'-B') Confocal-reconstructed transverse sections of the livers shown in (A-B). White dashed lines in (A-B') outline the livers. Yellow dashed lines in (A-B) mark the levels where the sections were reconstructed. (C-D) Distribution of hepatic biliary cells that express Alcam (red) and HSCs that express *Tg(hand2:*EGFP) (green). In wild-types (C), most HSCs (asterisk) are separated

from biliary cells (arrow) by hepatocytes (indicated by the bracket). In contrast, in *clo* mutant livers (D), HSCs are closely associated with biliary cells (arrows). (E) Numbers (mean±standard deviation) of hepatocytes and HSCs in wild-type and *clo* mutant larvae. Hepatocytes were detected by Prox1 staining (25). 4 wild-type and 4 *clo* mutant larvae were analyzed at 4 dpf. Asterisks indicate statistical significance: *$p < 0.05$; ***$p < 0.001$. (A-B, C-D) Confocal single-plane images, anterior to the top. Scale bars, 20 μm.

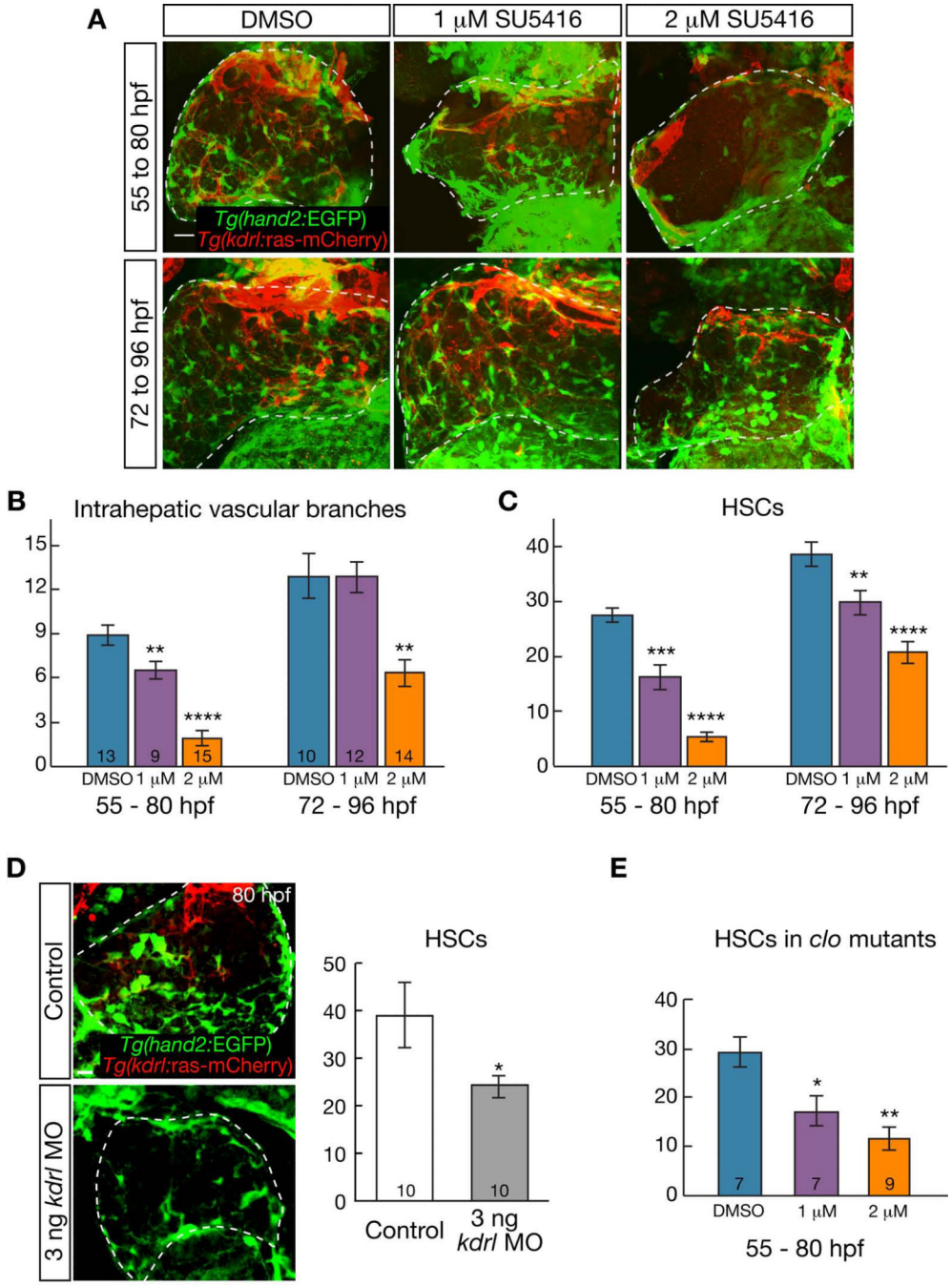

Fig. 6.

Inhibition of VEGF signaling during development decreases HSC number. (A-C) Inhibition of VEGF signaling reduced the number of intrahepatic vascular branches and HSCs in a dose and time-dependent manner. (A) Confocal projections of the livers in *Tg(hand2:EGFP; kdrl:ras-mCherry)* larvae that were treated with DMSO or the VEGF receptor inhibitor SU6415 from 55 to 80 hpf, or from 72 to 96 hpf. Dorsal views, anterior to the top. (B) Numbers (mean±SEM) of intraphepatic vascular branches in animals treated with DMSO, 1 μM SU6415, or 2 μM SU6415. (C) Numbers (mean±SEM) of HSCs in the same animals. (D) Knock-down of Kdrl levels resulted in a decrease in HSC number. Left panel shows confocal projections of the livers in uninjected controls and *kdrl* morpholino (MO)-injected

larvae at 80 hpf. Right panel shows the numbers (mean±SEM) of HSCs in uninjected controls and *kdrl*-knock down animals. (E) Numbers (mean±SEM) of HSCs in *clo* mutants treated with DMSO or SU5416. VEGF signaling inhibition decreased the number of HSCs in *clo* mutants. (A, D) White dashed lines outline the livers. Scale bars, 20 μm. (B-E) The numbers of animals analyzed are shown at the bottom of the graph. Asterisks indicate statistical significance: *$p < 0.05$; **$p < 0.01$; ***$p < 0.001$; ****$p < 0.0001$.

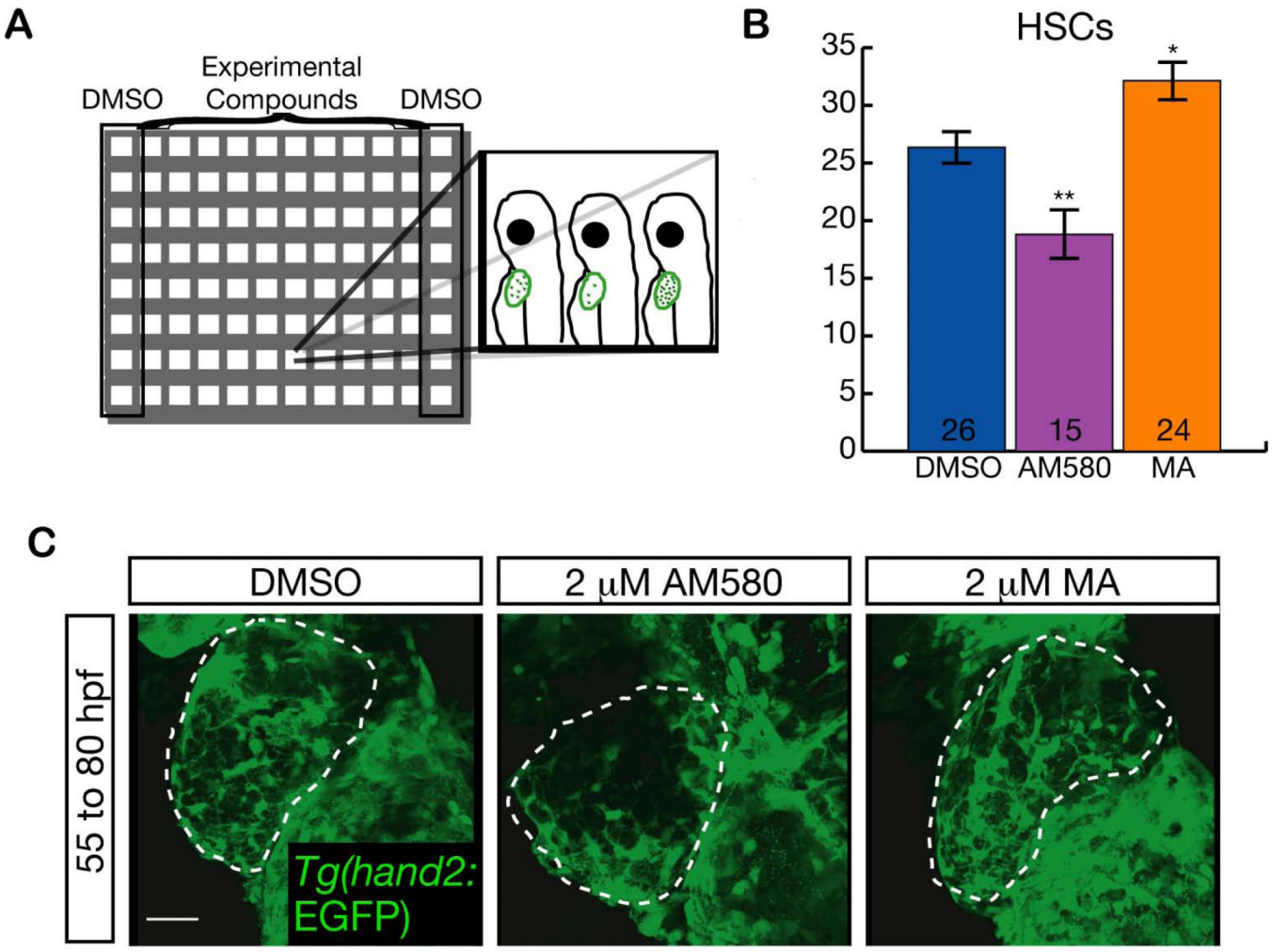

Fig. 7.

Chemical screen identifies compounds that alter HSC numbers. (A) Chemical screen set-up, with cartoon illustrating phenotypes of interest such as decreased HSC numbers (middle animal) and increased HSC numbers (right animal) compared to control (left animal). (B) Numbers (mean±SEM) of HSCs in animals treated with DMSO, AM580, or methoprene acid (MA). The numbers of animals analyzed are shown at the bottom of the graph. Asterisks indicate statistical significance: *$p < 0.05$; **$p < 0.01$. (C) Confocal projections of the livers in *Tg(hand2:EGFP)* larvae that were treated with DMSO, AM580, or MA from 55 to 80 hpf. Dorsal views, anterior to the top. White dashed lines outline the livers. Scale bars, 20 μm.